CC and MLO Compressions in Virtual Mammography with the Surface Evolver

M.Z. Nascimento, V. Ramos Batista

Abstract— This paper is a continuation of a long-term research devoted to Virtual Mammography, and here we give details already published in a previous short version. At the present stage we have obtained a fully virtual mammography procedure that faithfully reproduces all shapes of the breast and in its inside tracks the cancer at any step. The cancer is then precisely located for the surgery and can be removed through a small incision. So the whole structure is preserved and cured as an integral benefit to the patient. We utilise the Surface Evolver, a general purpose simulator that allows short codes and the addition of geometrical elements, which in our case represent different internal parts of the breast. Moreover, with a professional mammographer we studied CC and MLO compressions of a transparent breast phantom containing artificial nodules. Their displacements were tracked with a millimetre scale printed on a transparency sheet. Nodule displacements are ruled by physical and geometrical formulas that are now implemented in our simulator. In our first version they had not been equated yet. Here we describe how to derive these formulas. We have improved our virtual mammography procedure with the addition of geometrical elements and of equated nodule trajectories. This new version presents many progresses compared with our previous paper. Here we still work with the direct virtual mammography. In a forthcoming paper we shall present the reverse procedure, which starts from CC and MLO images that show a malignant tumour. Its coordinates will be given as the input for our simulator to output its correct location for the surgery, namely when the patient lies on the operating table.

Index Terms— Virtual Mammography, Surface Evolver, Computational Modelling, X-ray Images.

———————————————— ◆ ————————————————

1 INTRODUCTION

Mammographies are X-ray images of the breast under external compressions called Craniocaudal (CC) and Mediolateral Oblique (MLO). Together they can reveal the presence of nodules of tissues. Some nodules arise naturally and do not represent an abnormal formation. However, abnormal nodules appear as a reaction of the body against some instability in health. Such nodules are called tumours. In their turn, they can either stall and be harmless or spread and attack other cells. The first case is called benign and the second malignant, namely *cancer*.

In this last case the patient must have an operation. However, the mammographies show the breast in strongly deformed shapes. Cancer location is highly uncertain for the surgery, but still one can estimate it within a quarter of the breast. Depending on the kind of cancer the surgeon proceeds with quadrantectomy, a partial mastectomy authored by Umberto Veronesi, which we have already explained in [1].

Anyway, having one quarter of the structure removed is still traumatic for the patient. Ideally one should reduce this one quarter to almost the nodule dimensions. Now, all such nodules have a hard consistency but can be pretty small. The X-ray images should capture them with the best distinctness, which also helps classify them as Normal, Benign or Malignant.

If breast nodules were located with precision for the surgery the cancer could be removed through a small incision. After some slight corrections by plastic surgery the whole breast would remain preserved.

As a matter of fact, this is already possible through cutting-edge technologies like tomosynthesis [2], [3] and high-tech goggles for cancer detection [4]. There are may articles about these modern techniques but we cited just three for the sake of brevity. However, such techniques are quite expensive and still under improvement. Hence very few women can afford them in developing countries. Magnetic resonance could be a less dear alternative, but unfortunately not in poor countries yet.

The cheapest techniques are ultrasound and mammography. Both deform the shape of the breast considerably, but the latter has an advantage: not only the breast structure but also the mammography procedure can be modelled and simulated together in a totally virtual environment. Some related to softwares have been developed exactly with the purpose of locating nodules for the surgery. Here we cite [5], [6], [7], [8], [9], [10] and [11].

Unfortunately, they still present relevant limitations already discussed in [1] and [12]. To the best of our knowledge, until now, not one of them has been officially approved by a Medical Council as a reliable nodule locator permitting it to become part of surgical preparations.

In [1] and [12] we introduced the first part of a long-term research that aims at a full and detailed reproduction of the mammography procedure with the Surface Evolver [13]. Differently from previous works, our approach is to implement nodule trajectories under CC and MLO compressions in our model. These trajectories are studied by means of transparent

———————————————————
- *M.Z. Nascimento is a professor at FACOM-UFU, av. João Naves de Avila 2121, Bl.A, 38400-902 Uberlândia-MG, Brazil. E-mail: nascimento@facom.ufu.br*
- *V. Ramos Batista is a professor at CMCC-UFABC, av. dos Estados 5001, Bl.B, 09210-580 St. Andr´ e-SP, Brazil. E-mail: valerio.batista@ufabc.edu.br*

breast phantoms. See Figs. 1 and 2.

Fig. 1. Stereotactic Needle Biopsy,
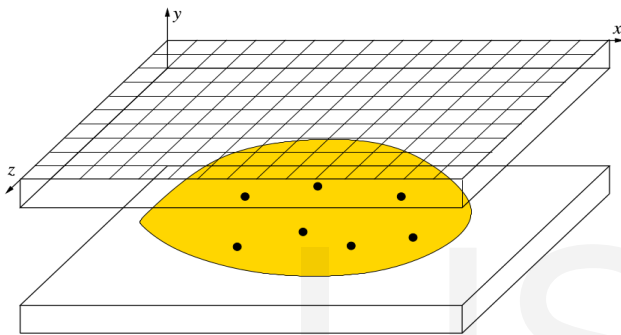www.cirsinc.com/products/all/44

Fig. 2. Performing CC/MLO compressions.

Compressions with the phantom were already performed and recorded in videos. Details are given in Subsection 3.2. Our modelling enables addition of structures that represent different tissues, muscles and glands in the breast. They can be either treated separately or as whole components, but we shall only adopt simplifications that do not cause relevant changes in the nodule trajectories.

One of the reasons for us to have chosen the Surface Evolver is that it enables to easily vary the complexity of the model. Another reason is the already built-in graphical environment and several Evolver functions, methods and command lines, all devoted to simulating physical experiments. Therefore, our source codes are relatively short, easy to handle and to understand.

This article is a continuation of [1]. Herewith we include the CC and MLO compres-sions with an internal structure and also give technical details. These were omitted in the short version [14].

2 MATERIALS AND METHODS

2.1 First Steps before CC and MLO Compressions

It is explained in [12] that our virtual mammography has 6 main steps named SRG (surgery), STU (stand-up), LAT (lay-on-table), CRC (cranio-caudal), LET (lean-on-table) and MLO

(medio-lateral-oblique). Fig. 3 shows important measurements of the initial positions. We always use the cgs-system. For CRC and MLO, measurements are taken directly from the X-ray images.
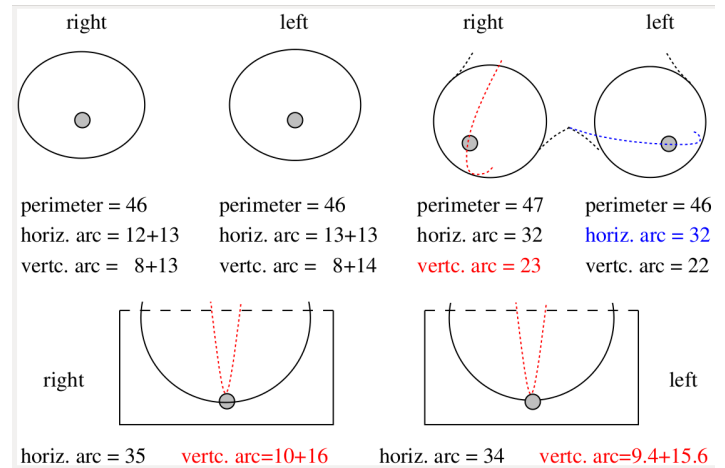

Fig. 3. Measurements of SRG, STU and LAT.

Fig. 4 shows important values at SRG deduced from Fig. 3. These are x_d, x_r, x_t, z_r, z_t and $brsep$, whose meanings are self-explanatory in Fig. 4.

Now we focus on SRG. Empirically, the breasts are within a range of the thorax that can be equated as a cylindrical surface called $bbase$ in our programs. However, the generatrix of $bbase$ cannot be taken as an ellipse, but as a *cubic ellipse* centred at ($-x_d$, $-z_t$):

$$\left| 1 + \frac{z}{z_t} \right|^3 + \left| \frac{x + x_d}{x_t} \right|^3 = 1.$$

Here the subscript t means "thorax", whereas d stands for "detachment". Namely, the generatrix of $bbase$ has a centre with x-coordinate detached from the portion of $bbase$ that is actually under the breast. More precisely, $x_d = x_r + brsep/2$.
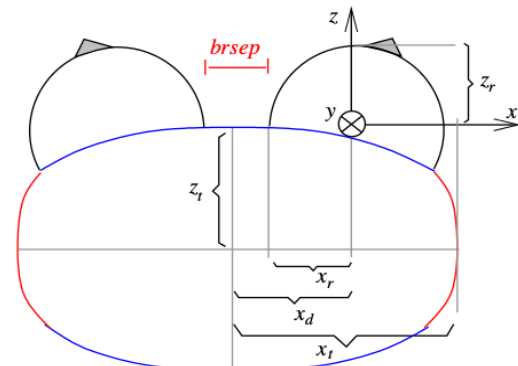

Fig. 4. Modelling the left breast by deduced unsigned values.

The breast surface is typically modelled as the upper hemisphere of an ellipsoid with the following radii: x_r, y_r and z_r. It

lies on *bbase* and z_r is also the 3rd coordinate of the nipple. In our case measurements indicate that $y_r = z_r = vtarc/\pi$, where *vtarc* stands for "vertic. arc" in Fig. 3. As depicted in Fig. 4, the upper blue arc that we call *fthrx* is almost straight. Therefore we take $x_r = (fthrx - bsep)/4$.

Although we use the half-ellipsoid approach to compute initial values of area and volume, breast and thorax meet at a contour that cannot be an ellipse. Empirically, it is also a cubic ellipse called bbcrc in our programs and equated as

$$(|x|/x_r)^3 + (|y|/y_r)^3 = 1.$$

We take $x_t = fthrx/1.7$ and $z_t = lthrx/1.7$, where the factor 1.7 is a rescaling of $\pi/2$. This one would be the factor if the generatrix of *bbase* were a circumference. Fig. 5 shows how we locate the nipple and place the lower plate for CC compressions.
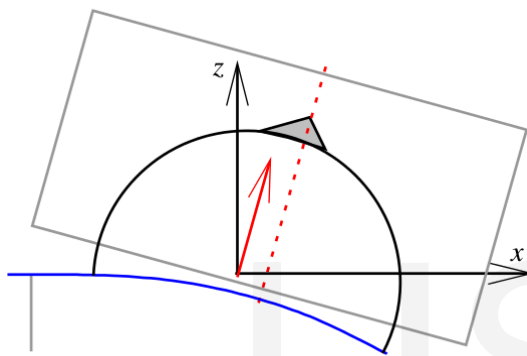

Fig. 5. Nipple and plate for CC.

The woman places her breast on the lower plate in such a way that most of it will lie thereon. We have observed it as a quite intuitive action. Fig. 5 shows the point of contact between the breast and the edge of the plate: it is at the origin of *Oxz*.

Of course, the edge of the lower plate is tangent to the thorax. In Fig. 5 we drew a red vector that is normal to the point of tangency. Let θ be the angle that this vector N makes with *Ox*. An easy computation gives $\theta = \arccos((x_d/x_t)^{3/2})$, whence

$$N = \left(z_t \cos^{\frac{4}{3}} \theta, \ 0, \ x_t \sin^{\frac{4}{3}} \theta \right). \tag{1}$$

Of course, the corresponding unitary normal is $n = N/|N|$.

Mammographers have standard plate dimensions: 18×24. For a better visualisation, however, our program shows plate dimensions that are closer to the patient's. In [1,12,14] we have used 12×18.

Now an important remark: bbcrc is used as a reference to obtain the values in Fig. 3. Namely, the tape-measure has to contour arcs of the breast with endpoints at *bbcrc*.

Our simulations with Evolver consider that *bbcrc* is fixed to the woman's thorax. This contour is easily recognised when the woman lies down. When she stands up, you can use the

jugular notch to locate it again.

But Fig. 5 indicates that part of the breast does not appear in the X-ray images. Namely, a priori we had better take LAT measurements only of its portion that actually lies on the lower plate. However, this procedure showed not to be practical, for one has to begin with the tape-measure at some point that is not between the breasts, and this point cannot be easily found.

We state it from personal experience: after many tries the corresponding LAT-values of *horiz.arc* in Fig. 3 were found to be 28.7 and 28 for the right and left breast, respectively. In CRC they are 32 and 33, respectively. This is consistent with the fact that compression widens the horizontal arc. In Fig. 3 they are greater because of the portions off the plate. These portions are both 18% for each breast, a percentage that from now on we shall consider as a standard.

Fig. 5 also indicates that the nipple lies at a point of the breast where the unitary normal η to the surface has the following property: its projection onto *Oxz* is parallel to *n*. Of course, this observation is empirical. Curiously, it holds for any of the 6 steps described above (from SRG to MLO).

Now we recall Fig. 3. For the left breast at SRG notice that *vtarc* = 8 + 14 from bottom to top. Let $n = (n_1, n_2, n_3)$, where in fact $n_2 = 0$. By taking this example our program will comb the breast surface until it finds the normal vector

$$\eta = \left(n_1, \ -n_3 \cos(\frac{8+11}{44} \cdot \pi), \ n_3 \sin(\frac{8+11}{44} \cdot \pi) \right). \tag{2}$$

The reader must be curious about the factor $(8 + 11)/44$ in (2). This should be 8/22 if at SRG the profile curve of the breast were an upper circumference. This is not quite the case (see Fig. 6). Hence we use the average between $8\pi/22$ and the right angle $11\pi/22$.
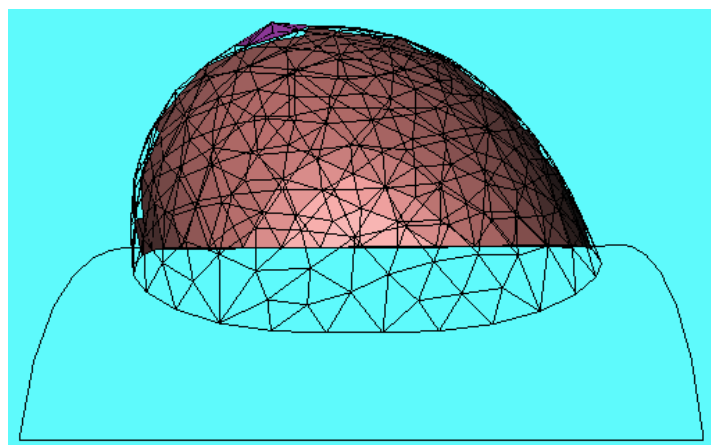

Fig. 6. Profile curve.

As explained in [12], we locate our coordinate system by

opening the back of the right hand upon the woman's sternum: Ox points as the thumb, Oy points as the other fingers, and the palm is raised along Oz. This procedure is the same for any of the 6 steps (from SRG to MLO). Taking this fact into account, it is still remarkable that η is again (2) at STU, LET and MLO. Of course, at LAT and CRC we have $\eta = n$.

The reader must be curious about how we control the effect of gravity, because our coordinate system $Oxyz$ moves with the patient. Evolver enables the determining and control of the gravitational field. However, what Evolver calls "gravity" is in fact the field $G = (G_1, G_2, G_3)$ that actually moves or deforms a body. For instance, at SRG the breast density ρ is the lowest one (about 0.5g/cm^3). Its effect is negligible in the z-direction, thus $G_3 = 0$. But the breast falls sideways, a fact empirically represented by $G_1 = 0.005$ and $G_2 = -0.015$ (for the left breast).

What deforms the breast is an energy E called Gravitational Potential Energy. For instance, the standard gravity in Evolver is $G = (0, 0, 1)$ instead of $(0, 0, -9.8)\text{m/s}^2$. Evolver does not work with unities, hence the user can fix any system of measurement and define the corresponding universal constants there. In our programs we use E with minus sign because Evolver inverts G automatically, but we want to simulate the direction of movement and deformation. Hence

$$E = -\iiint_B \rho \, G \cdot (x, y, z) \, dV, \tag{3}$$

where B is the whole breast, (x, y, z) are the spatial coordinates and dV is the volume element of integration. Since Evolver computes only surface integrals we have to determine a vector field F such that its divergent $\nabla \cdot F = G \cdot (x, y, z)$ (for constant ρ). By Gauß's Theorem, (3) is equivalent to

$$E = -\iint_{\partial B} \rho \, F \cdot n \, dS, \tag{4}$$

where ∂B is the surface of the breast and its base, and dS is the area element. We chose $F = (0, 0, F_3)$, $F_3 = z(G_1 x + G_2 y + G_3 z/2)$, where (x, y, z) are the spatial coordinates of n. Hence $\nabla \cdot F = G \cdot (x, y, z)$ as we wanted, with the advantage that (4) can be computed just over the surface of the breast because z is almost zero on its base.

2.2 Tracking Nodules

As explained in the Introduction, many softwares have been developed with the purpose of locating nodules for the surgery. However, some make simplifications that can compromise reliability while others go deeply into detailing. But this second approach leads to excessive computational complexity and the source codes tend to be untreatable.

With Evolver we can easily vary the complexity of the model, but always sticking to the essential. The resulting source codes are relatively short, easy to handle and to understand. As Evolver works with surface layers, our first approach is to mark a virtual nodule on a layer inside our model and track its trajectory. In Evolver we represent it by a black triangle. See Figs. 7 and 8.

Is the layer-approach reasonable? Well, there are many

kinds of breast tumours: lipoma (in the fat), carcinoma (in the glands), papilloma (inside the nipple), etc. In all cases they represent an abnormal group of cells of the corresponding component: fat, gland, lactiferous duct, etc. Therefore, a tumour cannot move about as if it were detached from its component. That is why we consider the layers as a reasonable approach.
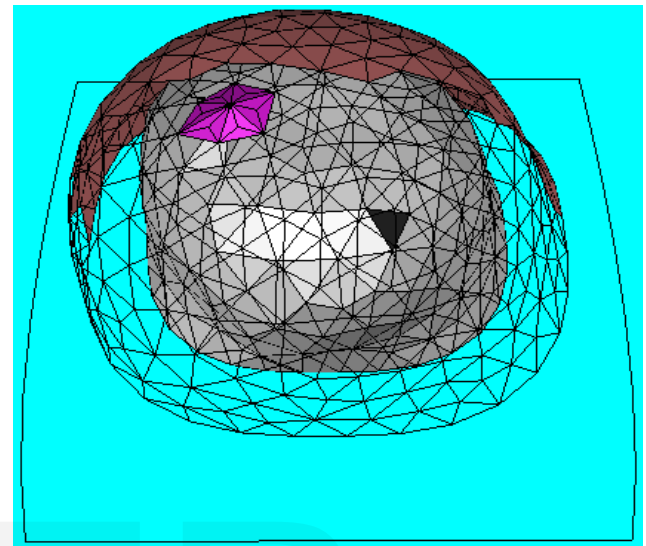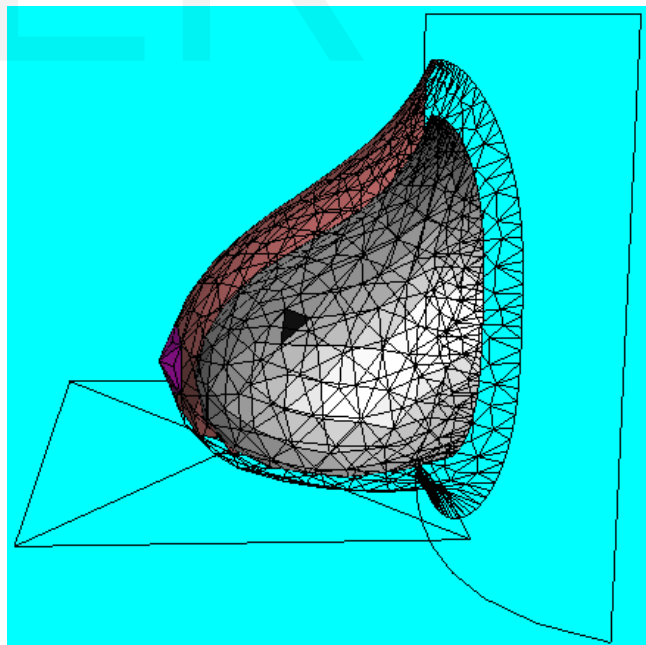

Fig. 7. Marking a nodule at SRG.

Fig. 8. Its position at LAT.

Although inexact, it is worthwhile to study the layer-approach before adding further complexity to our model. In Subsection 3.2 we compare Evolver's virtual displacement with actual displacements inside the phantom when it is compressed by a mammographer. Such tests are still at their beginning but

we have not found any inconsistency yet.

3 RESULTS

3.1 Performing CC and MLO Compressions

In Subsection 2.1 we explained that our initial values are based on approximations. For instance, by taking the vertical and horizontal arcs of the breasts as half-circumferences, from Fig. 3 we see that $y_r = z_r = vtarc/\pi$ ranges from 6.7 to 7.0 (right and left), and $x_r = hzarc/\pi$ ranges from 8.0 to 8.3. We call breast radius the mean of all such values. In our case it is $b_r = 7.50$.

When the woman's breast is placed against the lower plate, she intuitively chooses a point of contact with the edge. Her breast is then pushed upwards with the plate. We have observed that this point lies halfway along the lower vertical subarc (of 8cm in Fig. 3). Any geodesic from the base of the breast to the nipple is like an arc of circumference that measures $\pi/2$. Now halfway is $\pi/4$ and so the point of contact lies at a negative height on Oy given by $ngh = -b_r \cos(\pi/4)$. Together with Fig. 5 we then have a precise positioning of the plate with respect to $Oxyz$ for the CC compression.

Regarding MLO, we only need to rotate the plate by 45° about the line $(0, ngh, 0)+t\cdot n$, $t \in R$. Now the question is: To what extent do we compress the virtual breast? For the time being we apply fixed values observed in our example: a 4cm gap between the plates for the left breast and 5cm for the right one. The measurements taken of the X-ray images coincide with the corresponding ones obtained by our virtual tape-measure TMR (see [12] for details).

In our experiments we used a mammographer that displayed such a gap (see details in Subsection 3.2). Normally this piece of information is not printed on the X-ray images, but we suggest including it as part of future mammography procedures. Anyway, our TMR will always confirm measurements and can help establish the virtual gap.

Figs. 9 and 10 show the virtual mammographer compressions. As a matter of fact, only the final steps are illustrated here. Our program makes each compression gradually, and the user can follow the graphical output in real time.

For the time being our program is devoted only to the direct mammography procedure. Evolver cannot rewind simulations because its iterations strive for minimising the total energy, and each previous step is overwritten by the new one. The evolutions are not stored, for this would require too much memory. They could be saved in huge files, but these would be of little help due to the excess of information. Moreover, saving data all the time would make simulations too slow.

Of course, the importance of the virtual mammography resides in reversing its procedure. By starting from CC and MLO images that show a malignant tumour, we give its coordinates as the input. As the output we want its correct location at SRG, namely when the patient lies on the operating table. In Section 5 we present our strategies to deal with reversion in a future

work. As as matter of fact, we already have obtained some progress on reversion, and details can be found in [15]. Yet this reference is a short version with a third collaborator and still lacks some features commonly required for a patent.
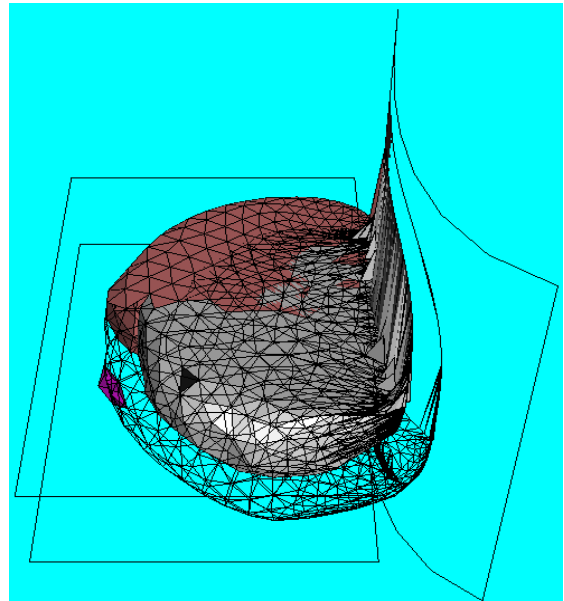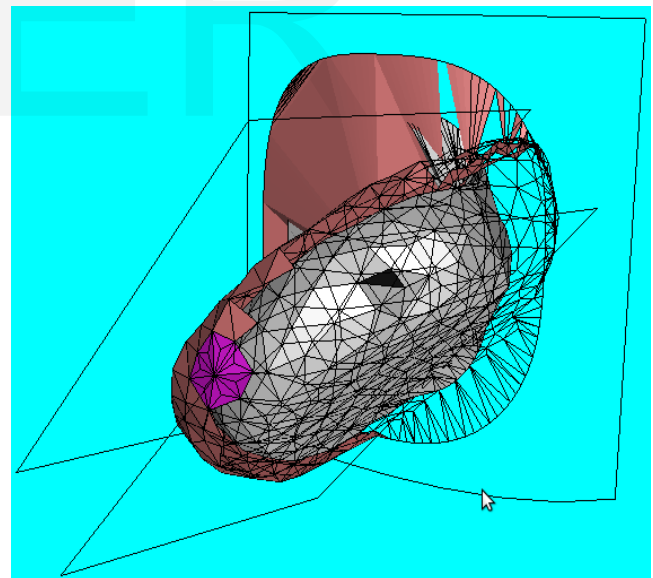

Fig. 9. CC with nodule.

Fig. 10: MLO with nodule.

3.2 Obtaining the Trajectories

The link Softwares of our home page

http://www.facom.ufu.br/~nascimento

contains five sample videos of tests with a transparent phantom. The phantom dimensions are compatible with the volunteer's, namely the one that we hypothesised in [1, 12]. A thor-

ough inspection of the videos enabled us to plot the nodule trajectories as shown in Fig. 11.
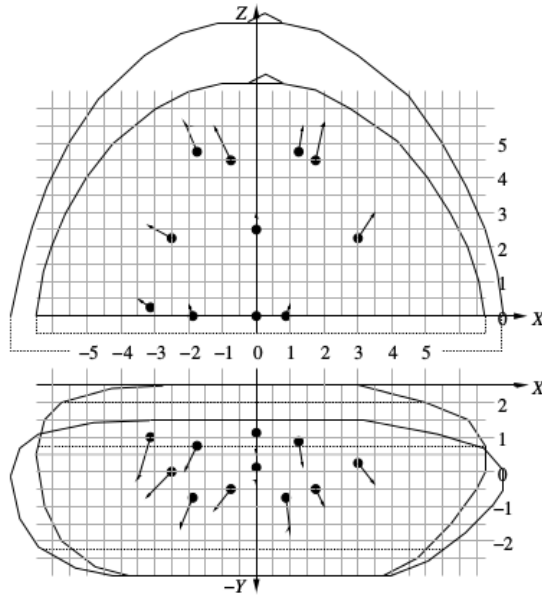

Fig. 11. Trajectories plotted on grid paper.

Our simulator tracks any chosen virtual nodule as depicted in Figs. 7 to 10. Its coordinates are saved in a file named `<pa-tient's number>Xtrj.st`, where `X=L,R` indicates either the left or the right breast, respectively. As an example, we have chosen a virtual nodule at SRG that lead to Table 1.

TABLE 1
TRAJECTORY OF A VIRTUAL NODULE

coord.	SRG	STU	LAT	CRC	LET	MLO
x	4.25	3.48	3.37	3.45	5.19	6.15
y	2.74	1.16	0.48	-1.31	1.15	0.65
z	3.12	2.53	2.70	5.00	3.82	4.63

At this point one must be careful before comparing Table 1 with Fig. 11. The videos show an upper plate which is like a tray, of which the borders are circa 8cm in height.

That is why the view from above shows the phantom reduced in scale. The same happens to the view from behind, which was recorded with the plastic millimetre sheet 8cm closer to the camera. By Fig. 12 there is a magnifying factor mf = 1.24 to be applied to Fig. 11.

But we take a greater Mf = 1.63 instead, because $2\,hzarc/\pi$ = 21.65 from Fig. 3 and the width is 13.25 in Fig. 11. This latter shows a nodule with coordinates $Mf \cdot (3.0, 0.25, 2.25)$ displacing to $Mf \cdot (3.5, -0.3, 3.0)$, namely

$$(4.90, 0.41, 3.67) + \Delta_{\text{phantom}} = (5.71, -0.49, 4.89). \quad (5)$$

Now, as explained in [12] our example is a breast that weighs 350 and has a volume varying from 700 at SRG to 660 at LAT. Hence the density of the phantom is nearly the double. The non-compressed phantom only represents a breast at LAT.

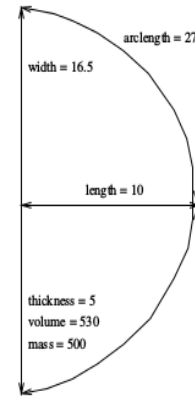At LET it practically does not change.

Fig. 12. Actual phantom dimensions.

Namely, the only columns of Table 1 that we can use are LAT and CRC. It seems to be of little use, but if our simulator behaves consistently with these two columns, then it can encourage the manufacturing of more complete breast phantoms for future comparisons.

Going back to Table 1, the transition from LAT to CRC gives

$$(3.37, 0.48, 2.70) + \Delta_{\text{breast}} = (3.45, -1.31, 5.00). \quad (6)$$

In practice the x-coordinate of (6) has not changed. Thus we shall not use it for comparisons. But both the y and z coordinates of the displacements Δ in (5) and (6) have grown consistently. Of course, in (6) they are the double of (5) but we recall that the phantom is 1.75 times denser than the breast.

Fig. 11 also shows that the phantom is compressed until reaching a gap of approximately 3cm between the plates. As commented in Subsection 3.1, we used a mammographer that displayed such a gap. This was also recorded in videos, as one can watch from our sample. They show a gap of 2.6cm, which multiplied by mf results in 3.22cm.

After some improvements in the program we shall be able to mark virtual nodules with precisely the same coordinates as the phantom's. Anyway, special care must always be taken with these comparisons. On the one hand, the phantom is actually used in propaedeutics and has uniform density. On the other hand, our model allows to add components with different densities, but we are still trying the layer-approach before assuming further complexities.

As a matter of fact, the experiments need phantoms that have elasticity, which is an important property of our anatomy. However, an artificial material satisfactorily close to the elasticity of the human breast is still unknown to us.

4 DISCUSSION

This work presents many progresses compared with our previous papers [1] and [12]. We have been dealing with the direct virtual mammography. However, as explained in Subsection

3.1, the most important is the reverse procedure. Our partial results constitute a long-term research, as remarked in [1], [12] and [14]. As shown in [15] the reverse procedure is still under implementation, and this forthcoming work will finally meet the requirements of a patent.

What are our strategies to implement it? As commented in Subsection 3.1, Evolver cannot rewind simulations because it always strives to minimise energy. But we have been taking this energy as the Willmore functional (see [12]). Therefore, if the human breast assumes a shape at rest that really corresponds to a minimised Willmore energy, then Evolver will strive to reach any of the 6 standard shapes no matter from which one we start.

For instance, from CRC to LAT we just release the upper plate and let Evolver minimise energy under the LAT-conditions. But even if it reaches a new LAT quite similar to the original one, they will not match exactly. Therefore, we need to perform several tests to see whether the backward way of the nodule is still close enough to the forward way.

In case they are not, then we shall adopt another strategy: 1) perform several direct virtual mammographies with a different nodule at each time; 2) collect all the trajectory files and interpolate the spatial points in each case; 3) find a general equation for a 3D-curve that will only depend upon the CC and MLO coordinates or 4) leave the trajectory files as a databank to help compute the spatial curve of any given initial data.

That is why we cannot dismiss the direct mammography yet. Of course, the phantom will be useful in any of these strategies even if it only represents LAT and CRC. Now, as explained in Subsection 2.1 we are still using the layer-approach. But how to know if this approach is satisfactory? We answer this question in the next section.

5 CURRENT & FUTURE DEVELOPMENTS

In future our software will work as follows: we start from CC and MLO images that show a tumour. The reverse procedure will locate it at SRG through the layer-approach. The location will be given in polar coordinates (r, p, d) centred at the nipple (see Figs. 13 and 14). The letters r, p and d stand for geodesic radius, phase and depth, respectively. For instance, with an eye pencil one can draw a coordinate system on the breast.

Now, the X-ray images are 2D-projections. How can they determine the spatial coordinates of the nodule? Projective Geometry cannot solve this problem because the breast is deformed in different ways. The answer resides in the size of the nodule in each X-ray view. Let us just give an example for the left breast. Roughly saying, a small picture of the nodule at MLO and a quite greater one at CC indicate that both p and d are close to zero. If it is the other way round, then $d \sim 0$ and $p \sim -\pi/2$. But the "third information" will in fact come from an accurate method that we shall develop in future.

The incision starts at (r, p) and then the scalpel cuts to depth

d. In case the tumour is found this will validate our software with the simplifications that we have been adopting. Otherwise the surgery will follow standard procedures. The software will then need further improvements like the addition of more complexity.
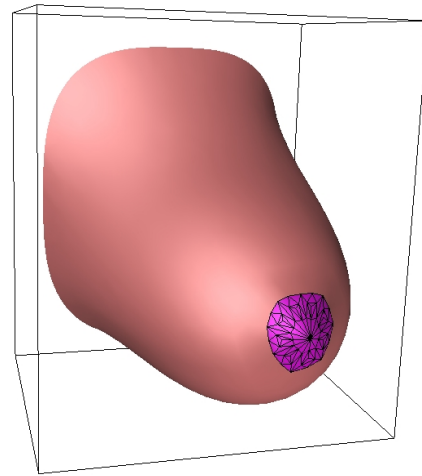

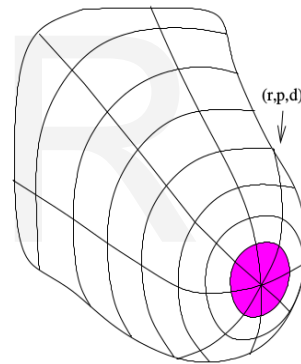Fig. 13. Patient's breast.

Fig. 14. Drawing polar coordinates on the breast.

6 APPENDIX

6.1 Surface Evolver 2.70 and Geomview 1.9.4

For the ones who prefer not to install these softwares, there is a virtual machine image called ubuntu11.10.ova available in the link Softwares of our homepage

http://hostel.ufabc.edu.br/~marcelo.nascimento

for download. In order to use it please follow the instructions in the Appendix of

http://arxiv.org/abs/1402.4101

Of course, the virtual machine is never as fast as our personal computer itself. Therefore, if the reader prefers to install the applications, we briefly describe it now. Regarding Geomview, you can easily install after downloading it from http://www.geomview.org. Linux has the very practical command line sudo apt-get install geomview, which however does not always load the most recent

version. Namely, for Evolver it installs the version 2.30, but this unfortunately will not run our present datafiles.

While apt-get does not work for Evolver 2.70, you can install it manually. Go to Ken Brakke's home page http://www.susqu.edu/brakke and click on the Evolver link. There you will find installation instructions for Linux, but they are rather general. In the case of Ubuntu 11.10 and 12.04, after you download evolver-2.70.tar.gz and extract it in your Desktop, access synaptic to install the packages freeglut*, libxi-dev, libxmi-dev and libxmu-dev. It is possible that you do not have some of them in synaptic. In this case, install them manually. For example, get libxmi-1.2.tar.gz from http://www.filewatcher.com and then right-click on it to open with Ubuntu Software Centre.

By proceeding with the general instructions, now access the directory evolver-2.70/src in order to overwrite the file extern.h with its namesake available on our homepage. Then open Makefile with a text editor and remove # from lines 64-66, namely

CFLAGS= -DLINUX -DOOGL -DPTHREADS
GRAPH= glutgraph.o
GRAPHLIB= -lGL -lGLU -lglut -lpthread

and finally from line 70:

GRAPHLIB= -lGL -lGLU -lglut -L/usr/X11R6/lib -lXi -lXmu -lpthread

Save Makefile and then run make.

Now you will be able to locally run Evolver in the scr-directory. For instance, at the terminal prompt enter ./evolver ../fe/cube and follow the instructions from pages 16-18 of manual270.pdf (included in the above tar-file).

In order to call evolver at any sub-directory, first you will have to locate it. Open a terminal window, type locate evolver and press the Enter key. A long list will be printed on the screen. Scroll it and you will find a path like, for instance

/usr/local/evolver-2.70/src/evolver

Now you will probably have to become superuser. Then copy this path and paste it at the prompt within the following command:

ln -s /usr/local/evolver-2.70/src/evolver /bin/

Notice that there must be an empty space between the words evolver and /bin/. Press the Enter key, and right afterwards Evolver will then be recognised globally. If you already have a symbolic link to an older version, say 2.50, please unmake it before creating the new link. For instance, type

unlink /usr/local/evolver-2.50/src/evolver

Afterwards, again as superuser, remove the file evolver in the directory bin. Then create the new link as explained above.

ACKNOWLEDGMENT

REFERENCES

[1] M. Z. do Nascimento and V. Ramos Batista, "First Steps to Virtual Mammography with the Surface Evolver," *Recent Patents on Medical Imaging*, vol. 4, no. 2, pp. 87–94, 2014.

[2] S. Ciatto, N. Houssami, D. Bernardi, F. Caumo, M. Pellegrini, S. Brunelli, P. Tuttobene, P. Bricolo, C. Fantò, M. Valentini, "Integration of 3D Digital Mammography with Tomosynthesis for Population Breast-Cancer Screening (Storm): a Prospective Comparison Study," *The Lancet Oncology*, vol. 14, no. 7, pp. 583–589, 2013.

[3] P. Skaane, A. I. Bandos, R. Gullien, E. B. Eben, U. Ekseth, U. Haakenaasen, M. Izadi, I. N. Jebsen, G. Jahr, M. Krager, "Comparison of Digital Mammography Alone and Digital Mammography Plus Tomosynthesis in a Population-Based Screening Program," *Radiology*, vol. 267, no. 1, pp. 47–56, 2013.

[4] Y. Liu, W. J. Akers, A. Q. Bauer, S. Mondal, K. Gullicksrud, G. P. Sudlow, J. P. Culver and S. Achilefu, "Intraoperative Detection of Liver Tumors Aided by a Fluorescence Goggle System and Multimodal Imaging," *Analyst*, vol. 138, no. 8, pp. 2254–2257, 2013.

[5] S. N. Bhatti and M. Sridhar-Keralapura, "A Novel Breast Software Phantom for Biomechanical Modeling of Elastography," *Medical Physics*, vol. 39, no. 4, pp. 1748–1768, 2012.

[6] K. Bliznakova, Z. Bliznakov, V. Bravou, Z. Kolitsi, and N. Pallikarakis, "A Three-Dimensional Breast Software Phantom for Mammography Simulation," *Physics in Medicine and Biology*, vol. 48, no. 22, pp. 3699–3721, 2003.

[7] C. M. Hsu, M. L. Palmeri, W. P. Segars, A. I. Veress and J. T. Dobbins III, "An Analysis of the Mechanical Parameters Used for Finite Element Compression of a High-Resolution 3D Breast Phantom," *Medical Physics*, vol. 38, no. 10, pp. 5756–5770, 2011.

[8] M. Kuhlmann, E. Fear, A. Ramirez-Serrano and S. Federico, "Mechanical Model of the Breast for the Prediction of Deformation During Imaging," *Medical Engineering & Physics*, vol. 35, no. 4, pp. 470–478, 2013.

[9] R. M. Nishikawa, "Current Status and Future Directions of Computer-Aided Diagnosis in Mammography," *Computerized Medical Imaging and Graphics*, vol. 31, no. 4, pp. 224–235, 2007.

[10] P. Pathmanathan, D. J. Gavaghan, J. P. Whiteley, S. J. Chapman and J. M. Brady, "Predicting Tumor Location by Modeling the Deformation of the Breast," *Biomedical Engineering*, vol. 55, no. 10, pp. 2471–2480, 2008.

[11] J. Tang, R. M. Rangayyan, J. Xu, I. El Naqa and Y. Yang, "Computer-Aided Detection and Diagnosis of Breast Cancer with Mammography: Recent Advances," *Information*

Technology in Biomedicine, IEEE Transactions on, vol. 13, no. 2, pp. 236–251, 2009.

[12] M. Z. do Nascimento and V. Ramos Batista, "Simulating External Compressions of the Breast with the Surface Evolver," *Journal of Physics: Conference Series*, vol. 490, p. 012146, 2014.

[13] K. A. Brakke, "The Surface Evolver," *Experimental Mathematics*, vol. 1, no. 2, pp. 141–165, 1992.

[14] M. Z. do Nascimento and V. Ramos Batista, "Simulating CC and MLO Compressions with the Surface Evolver," *Journal of Physics: Conference Series*, vol. 574, p. 012072, 2015.

[15] A. Fabris, M. Z. do Nascimento and V. Ramos Batista, "A Software Tool Based on the Surface Evolver for Precise Location of Tumours as a Preoperative Procedure to Partial Mastectomy," *Journal of Physics: Conference Series*, vol. 633, p. 012132, 2015.